Preparation and Properties of Deep Dye Fibers from Poly(ethylene terephthalate)/SiO_2 Nanocomposites by *In Situ* Polymerization

Yongzhe Yang, Hongchen Gu

National Key Laboratory of Nano/Micro Fabrication Technology, Key laboratory for Thin Film and Microfabrication of Ministry of Education, Institute of Micro and Nano Science and Technology, Shanghai Jiao Tong University, Shanghai 200030, China

Received 9 July 2005; accepted 30 August 2005
DOI 10.1002/app.23069
Published online 26 April 2007 in Wiley InterScience (www.interscience.wiley.com).

ABSTRACT: In this study, poly(ethylene terephthalate) (PET)/SiO_2 nanocomposites were synthesized by *in situ* polymerization and melt-spun to fibers. The superfine structure and properties of PET/SiO_2 fibers were studied in detail by means of TEM, DSC, SEM, and a universal tensile machine. According to the TEM, SiO_2 nanoparticles were well dispersed in the PET matrix at a size level of 10–20 nm. The DSC results indicated that the SiO_2 nanoparticles might act as a marked nucleating agent promoting the crystallization of the PET matrix from melt but which inhibited the crystallization from the glassy state, owing to the ''crosslink'' interaction between the PET and SiO_2 nanoparticles. The tensile strength of 5.73 MPa was obtained for the fiber from PET/0.1 wt % SiO_2, which was 17% higher than that of the pure PET. The fibers were treated with aqueous NaOH. SEM photographs showed that more and deeper pits were introduced onto PET fibers, which provided shortcuts for disperse dye and diffused the reflection to a great extent. According to the *K/S* values, the color strength of the dyeing increased with increasing SiO_2 content. It is found that the deep dyeability of PET fibers was improved greatly. © 2007 Wiley Periodicals, Inc. J Appl Polym Sci 105: 2363–2369, 2007

Key words: poly(ethylene terephthalate); SiO_2; fibers; nanocomposites; nanoparticles; deep dye; *in situ* polymerization

INTRODUCTION

Poly(ethylene terephthalate) (PET) commonly used for textile application represents the largest percentage among synthetic fibers in the market, and is used as pure material or mixed with cellulose. To have a better appearance and utilization, addition of dyes in the manufacturing process is required. PET has the most compact and crystalline structure, and is markedly hydrophobic. Its structure nature can be a disadvantage for dyeing.[1–5]

Because of the importance of PET fibers to the textile industry, researchers are very much interested in improving their dyeing properties. Several authors have studied the effects of modifying agents, dyeing conditions, and dyeing processes of dispersed dyes for PET fibers.[6] Shukla et al. reported that organic compounds, called carriers (phenols, amines, aromatic hydrocarbons, esters, etc.), which are rapidly absorbed, have been used to accelerate the dyeing rate. But many effective carriers are also suspected environmental hazards.[7–11] Thakore et al. reported a dyeing process using ultrasonic to form and break small bubbles, making the dyeing better at low temperatures achieving levels comparable with dyeing at boiling using carriers.[12–16] Knittel et al. reported that PET fibers could be dyed using carbon dioxide in supercritical state as solvent, avoiding the water pollution and the need of drying with excellent firmness levels.[3,17,18]

In this article, we have demonstrated that it is possible to improve the dyeability of PET fibers modified with inorganic nanoparticles, which has been paid little attention to before. We adopted *in situ* polymerization for realizing real nanocomposites by nanoscale. This methodology consists of dispersing the inorganic nanoparticles into the monomers; then the mixture is polymerized by adding the catalyst agent under certain condition. The properties of PET fibers, both unmodified and modified with SiO_2 nanoparticles, have been studied by means of TEM, DSC, SEM, and a universal tensile machine.

EXPERIMENTAL

Materials

Nano-SiO_2 with an average particle size of 10 nm was supplied by Yuda Chemical (Zhejiang, China). Ethyl-

Correspondence to: H. Gu (hcgu@sjtu.edu.cn).
Contract grant sponsor: State Development Planning Commission of China; contract grant number: 2001BA310A10.
Contract grant sponsor: Shanghai Nano Technology Project of China; contract grant numbers: 0213nm002, 0352nm023.

ene glycol (EG), terephthalic acid, trimethyl phosphate, Sb_2O_3 (as catalyst), NaOH, CTAB, and organosilane were supplied by Chemical Reagents (China).

Preparation of the SiO_2/EG sol

About 2.4 g of organosilane was dissolved in 100 mL water and heated at 333–343 K for 20 min. The solution was added dropwise to 100 g 25 wt % SiO_2 sol by separating funnel, maintaining the flow rate at 10 mL/min. Then the modified SiO_2 was transferred from water to EG by rotatory evaporation. The dispersion of 25 g of modified SiO_2 in a 100 mL of EG solution was added to 100 mL of EG which was heated at 353–393 K. Similarly, the flow rate was controlled at 10 mL/min. The mixture was stirred vigorously for 30 min.

Preparation of PET/SiO_2 nanocomposites by *in situ* polymerization

PET pellets with varied content of SiO_2 were prepared by the terephthalic acid route. In a 5-L cylindrical reactor, 1 kg of EG (16.1 mol) and varied content of SiO_2 were placed; the mixture was stirred for 0.5 h at room temperature. Then 2 kg of terephthalate (12.0 mol), a few drops of trimethyl phosphate, and some Sb_2O_3 were added, with vigorous stirring to obtain a homogeneously dispersed system. The SiO_2 contents of the PET nanocomposites are shown in the Table II. The esterification was carried on at 523–533 K and polycondensation at 533–543 K. After 3–4 h polycondensation, the melting polymer was extruded through an orifice at nitrogen pressure of 3.0 kg and cooled with water.

Melt spinning

PET/SiO_2 pellets were subjected to melt spinning using a spinning instrument ABE-25 equipped with a spinneret with thirty-six nozzles of 0.3 mm diameter. The temperatures of screw extruder were set at 558, 568, 573, and 573 K, respectively. The drawing of the fibers was carried out on a Barmag 3013 drawing device with draw ratio 3.7.

Characterization

PET/SiO_2 nanocomposite specimens were sliced at 193 K with an Ultracut Uct microtome. A transmission electron microscope was operated at 75 kV. Before TEM experiment, specimens were annealed in a vacuum oven at 473 K for 1 week to remove moisture completely.

The crystallization behaviors of the samples were examined using Perkin–Elmer differential scanning calorimeter DSC-7. Samples were heated at 20 K/min to 573 K, maintaining 573 K for 5 min to eliminate the thermal and shear history effects, then cooled at 20 K/min to 373 K, and heated at 20 K/min to 573 K again. The peak corresponding to the maximum in the heat flow rate was taken as the crystallization temperature (T_c).

Tensile properties of PET/SiO_2 fibers were measured using an AGS material testing machine with gauge length of 250 mm at a crosshead speed of 500 mm/min. The elongation at break and tensile strength were obtained by averaging at least 10 trials of the tensile test for each sample.

Alkaline (NaOH) hydrolysis was performed in one bath (373 K) with the catalyst (CTAB) for 20 min. A soup washing (358 K) and then warm water washing, dilute acetic acid washing, and cold water washing were performed until the fibers were in a neutral situation. Weight loss (WL) of the fibers was calculated as follows:

$$WL(\%) = [(W_0 - W_1)/W_0] \times 100$$

where W_0 and W_1 are fiber weights before and after hydrolysis, respectively.

Surfaces of alkaline hydrolyzed fibers were observed with a JEOL JSM-6340F field emission scanning electron microscopy.

The fibers were dyed with 5% of the weight of the fibers of Disperse Blue (Foron Blue RD-S) at a liquor ratio of 1 : 100. The samples were introduced into the dye bath at 333 K, then the temperature was gradually raised up to boiling point within 20 min, and then dyeing was continued for 30 min with stirring. The dyed samples were rinsed with cold water, then soaped with a solution contained no-ionic detergent (2 g/L), at 371 K for 15 min, and rinsed with tap water. The depth of the color was evaluated by the *K/S* value (where *K* is the absorbency factor of the colored substance and *S* is the scattering factor), which was tested with a Hitachi Type 330 spectrophotometer (Tokyo, Japan) ($\lambda = 565$ nm).

RESULTS AND DISCUSSIONS

The dispersion of nanoparticles in PET/SiO_2 nanocomposites

It is well known that the dispersion of nanoparticles in the polymer matrix has a significant impact on the properties of composites.[19–21] As the nanoparticles have a strong tendency to agglomerate, homogeneous dispersion of the nanoparticles in the polymer has been considered as a difficult process. A good dispersion may be achieved by surface modification of the nanoparticles under an appropriate processing condition.[22] In this work, a novel approach has been utilized to disperse nanoparticles in the PET matrix.

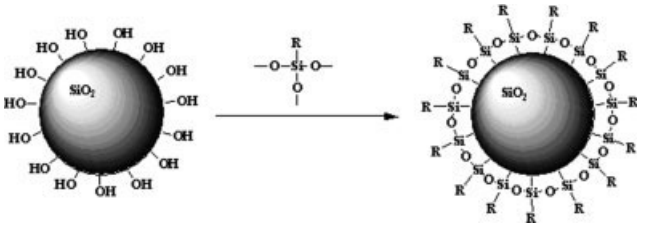

Figure 1 Formation of an organosilane monolayer on the surface of a SiO_2 nanoparticle.

First, to disperse the nanoparticles in the EG, the SiO_2 surface was modified by organic compound. The introduction of coupling agent onto SiO_2 surface was achieved by reaction described in Figure 1.

Figure 2 shows TEM image of PET-based nanocomposite having 2.0 wt % of SiO_2 nanoparticles prepared by *in situ* polymerization, where the dark areas represent the SiO_2 particles and gray/white areas represent the PET matrix. It is clearly seen in Figure 2 that SiO_2 nanoparticles with a diameter 10–20 nm were dispersed uniformly in the matrix, which resulted from the introduction of the specific dispersion agent on the SiO_2 surface.

Thermal behavior of PET/SiO_2 fibers

The main parameters of nonisothermal crystallization of pure PET and PET/SiO_2 fibers are listed in Table I. The inherent viscosities of all samples were maintained nearly the same (0.67–0.68) prior to the study. PET/SiO_2 fibers showed higher melt-crystalline temperature (T_c) by about 11.5–13.4 K and melt-crystalline heat (H_c) by about 2.9–4.3 J/g in comparison with pure PET fiber. This could be attributed to the incorporation of effective nucleation agent SiO_2 and its satisfactory dispersion in the PET matrix. It is well known that the molecular chains of pure PET present higher inflexibility and less mobility. As a result, both growth rate and nucleation rate are very slow, corresponding to the low T_c and H_c. When a small amount of SiO_2 nanoparticles was added to the PET matrix, it enhanced the crystallization of PET by providing large numbers of nucleation sites. The molecular chains can crystallize at high temperature and tend to transform perfectly at the same time. Both growth rate and nucleation rate were very fast, corresponding to the high T_c and H_c. However, with increasing SiO_2 content, excessive nanoparticles restricted the motions of the PET molecular segment and prohibited the growth rate of PET crystallites, owing to a strong interaction between the SiO_2 nanoparticles and PET worked as

TABLE I
The Main Parameters of Nonisothermal Crystallization of all PET Fibers

Specimen	T_g (K)	T_c (K)	T_m (K)	H_c (J/g)	ΔT_{sc} (K)
Pure PET	340.7	468.4	519.4	38.6	51.0
PET/0.1 wt % SiO_2	347.4	479.9	526.8	41.5	46.9
PET/0.5 wt % SiO_2	350.9	481.8	524.6	42.9	42.8
PET/2.0 wt % SiO_2	352.5	480.3	524.9	42.0	44.6

T_g, glass transition temperature; T_c, melt-crystalline temperature; T_m, equilibrium melting temperature; H_c, melt-crystalline heat; $\Delta T_{sc} = (T_m - T_c)$, degree of supercooling.

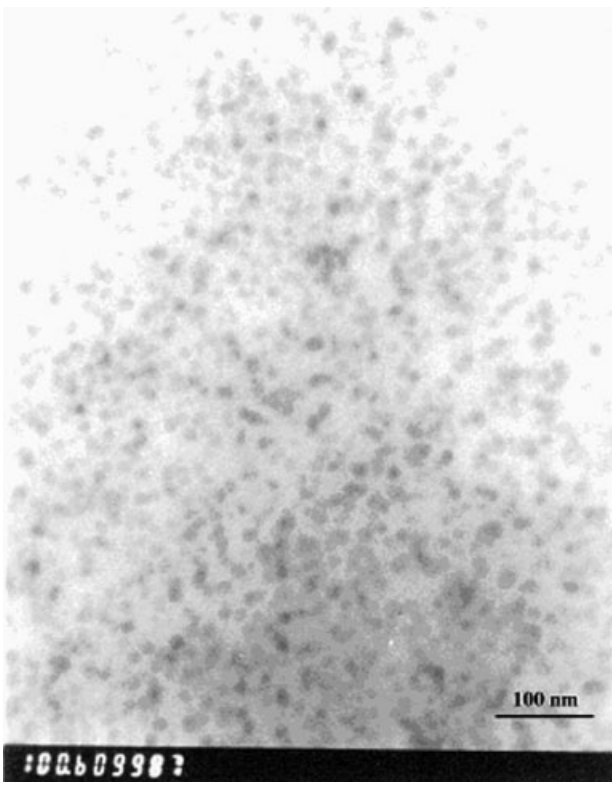

Figure 2 TEM photograph of PET/2.0 wt % SiO_2 nanocomposite.

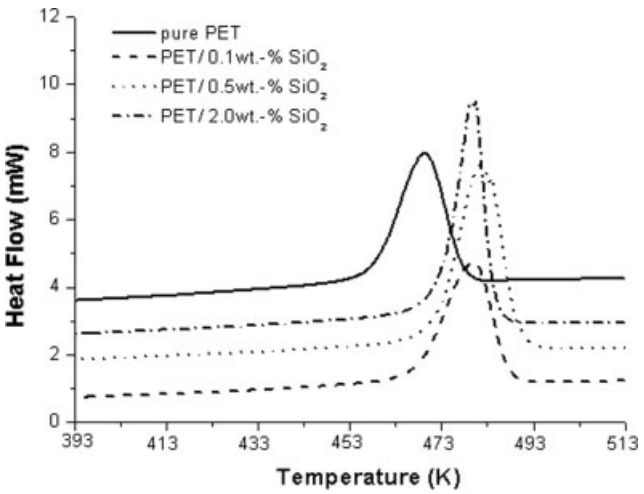

Figure 3 DSC cooling scans of nonisothermal crystallization from melt state for pure PET and PET/SiO_2 fibers.

TABLE II
Mechanical Properties of PET/SiO_2 Fibers (DR = 3.7)

Specimen	Ultimate stress (*N*)	Elongation at break (%)	Tensile strength (MPa)	Initial modulus (MPa)
Pure PET	3.85	32.60	4.90	113.36
PET/0.1 wt % SiO_2	3.99	35.69	5.73	124.19
PET/0.5 wt % SiO_2	3.85	34.47	5.25	113.48
PET/2.0 wt % SiO_2	3.01	28.53	4.05	108.49

crosslinked points of the PET molecular network. Therefore, the T_c of PET fibers reached the temperature of 481.8 K, and then began to decrease. Figure 3 shows the DSC cooling scans of crystallization from melt state for pure PET and PET/SiO_2 fibers. The temperatures of peaks varied with the content of SiO_2 and their shapes become much narrower and higher than that of pure PET.

From Table I, the T_g of pure PET is about 340.7 K, in agreement with previous reported data, whereas higher values were observed for all modified fibers.[23] It is believed that the SiO_2 nanoparticles might act as a ''bridge,'' owing to the existence of the ''crosslinking'' interaction between PET matrix and SiO_2 nanoparticles, which restricted the flexibility of PET molecular chains from the glassy state. The T_g of the PET fibers increased linearly with increasing SiO_2 content.

Generally, the melting temperature (T_m) can reflect the thermal properties of fibers. In other words, the excellent thermal dimensional stability is reflected in T_m. It is shown in Table I that the melting temperature of PET/SiO_2 fibers was 5.2–7.2 K higher than that of pure PET fibers, which implied that the PET/SiO_2 fibers were more stable.

Mechanical properties of PET/SiO_2 fibers

Addition of SiO_2 nanoparticles had an influence on the mechanical properties, as shown in Table II. It can be seen that the effect of SiO_2 nanoparticles on the mechanical properties of PET fibers is very distinct and the composition dependence is pronounced. The tensile strength of PET fibers changed nonlinearly with respect to the SiO_2 content. As the SiO_2 content increased, the tensile strength of PET/SiO_2 fibers reached a value of 5.73 MPa, which was 17% higher than that of pure PET fibers (4.90 MPa). This enhancement of the tensile strength is ascribed to a strong interaction between the SiO_2 nanoparticles and PET matrix, which worked as crosslinked points of the PET macromolecular network. These similar physical crosslinked points made the macromolecular network more complete and effectively enhanced stress resistance. However, a gradual declination in the tensile strength is observed after that, owing to the weakened H-bonding interactions between the PET chains and the presence of more voids provided by excessive amounts of SiO_2 nanoparticles acting as stress concentrating defects. Consequently, the imperfect interface could not sustain the large interfacial shear stress. In the case of PET/2.0 wt % SiO_2 fiber, it had a tensile strength of 4.05 MPa, lower by about 17% than that of pure PET fiber.

In addition to having the nonlinear change in the tensile strength, the initial modulus and elongation at break of the PET/SiO_2 fibers behaved in the same way with increasing the addition of SiO_2 from 0 to 2.0 wt %.

Alkaline hydrolysis of PET/SiO_2 fibers

Table III shows the effect of the alkaline hydrolysis on WL of pure PET and PET/SiO_2 fibers. Some authors assumed linear time dependence of WL,[24,25] whereas others found an exponential function to better fit the experimental data.[26,27] In this study, we observed that WL increased nonlinearly with hydrolysis time. For the pure PET fibers, the estimated regression equation between %WL and time (t) is $\%WL = 3.24 \times t^{0.67}$ (correlation coefficient $R^2 = 0.995$). In contrast, for PET/SiO_2 fibers, the regression equations are $\%WL = 3.41 \times t^{0.67}$($R^2 = 0.996$), $\%WL = 3.29 \times t^{0.68}$($R^2 = 0.998$), and $\%WL = 2.67 \times t^{0.78}$($R^2 = 0.992$) at SiO_2 content of 0.1, 0.5, and 2.0 wt %, respectively.

All WLs increased with increasing hydrolysis time, as shown in Table III. The rate of hydrolysis increased in the order pure PET < PET/0.1 wt % SiO_2 < PET/0.5 wt % SiO_2 < PET/2.0 wt % SiO_2, pure PET showing slowest loss in weight during the whole treatment process. Hydrolysis appeared to develop preferen-

TABLE III
Weight Loss of PET/SiO_2 Fibers at Different Hydrolysis Time

Sample	Weight loss (%) (min)					
	10	20	30	40	50	60
Pure PET	13.6	25.0	31.8	41.1	45.1	49.8
PET/0.1 wt % SiO_2	14.1	25.3	33.6	41.3	45.3	51.2
PET/0.5 wt % SiO_2	14.9	25.8	34.1	41.7	45.9	54.2
PET/2.0 wt % SiO_2	16.3	26.7	34.8	49.2	57.9	61.6

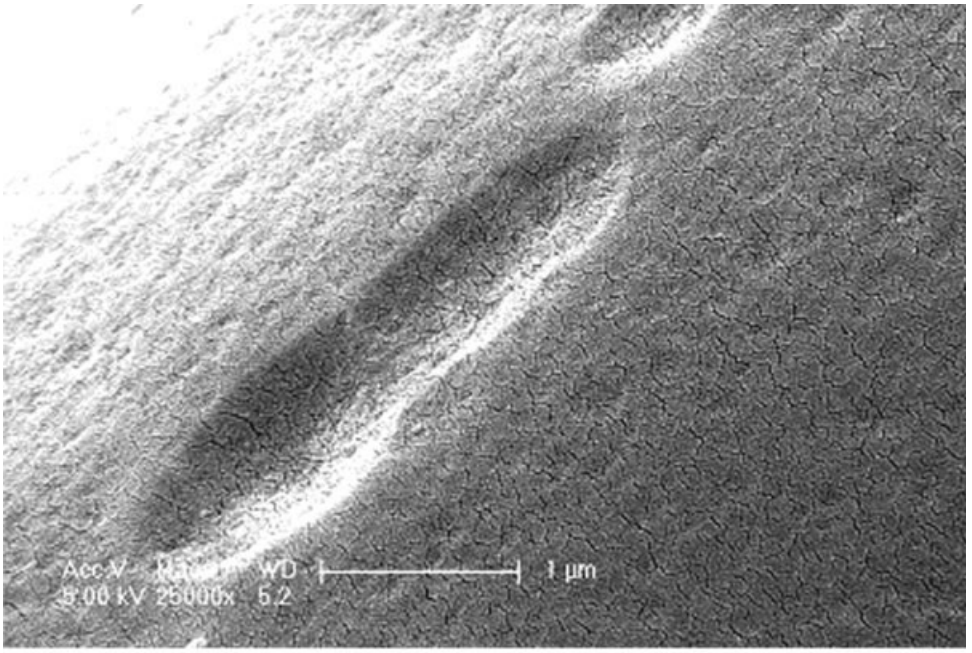

(a)

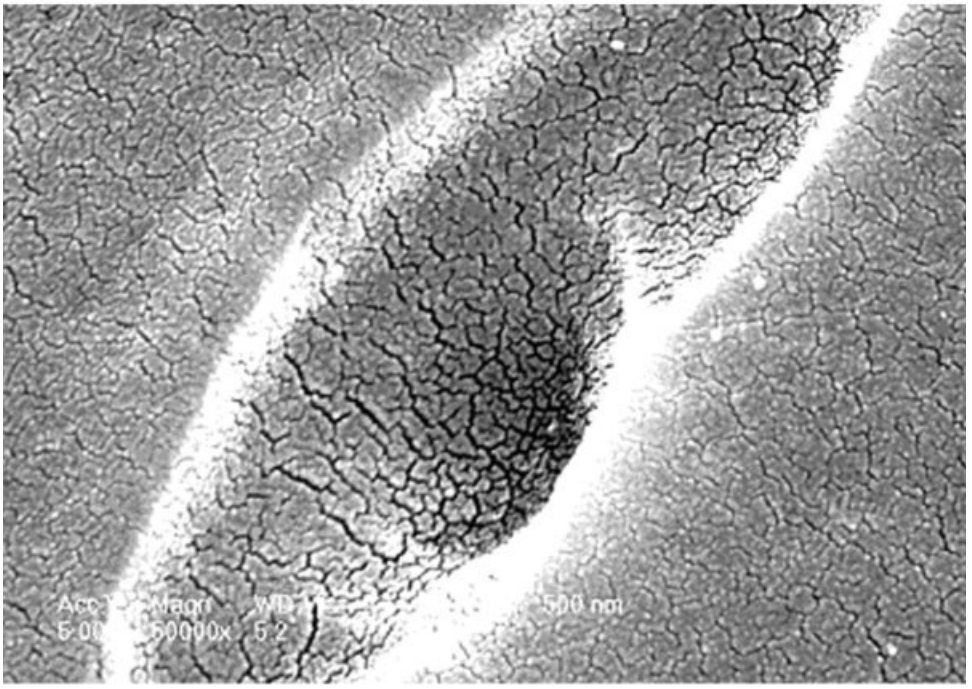

(b)

Figure 4 SEM photos of alkaline hydrolyzed fiber surface for pure PET.

tially around the SiO_2 nanoparticles, location known to be of lower crystallinity.[28] More SiO_2 nanoparticles were exposed as PET degraded around them. WL of PET/2.0 wt % SiO_2 was almost the same as that of PET/0.1 wt % SiO_2 or PET/0.5 wt % SiO_2 initially but later (after 30 min) increased rapidly, as a result exposing more inner weak points formed within 30 min treatment.

SEM

SEM photographs in Figures 4 and 5 describe the surface morphologies of alkaline hydrolyzed PET fiber. As is well known, the surface of the pure PET fiber without alkaline hydrolysis is smooth and highly compact.[5] However, there were a lot of irregular micropits on the surface of the fiber etched in aqueous

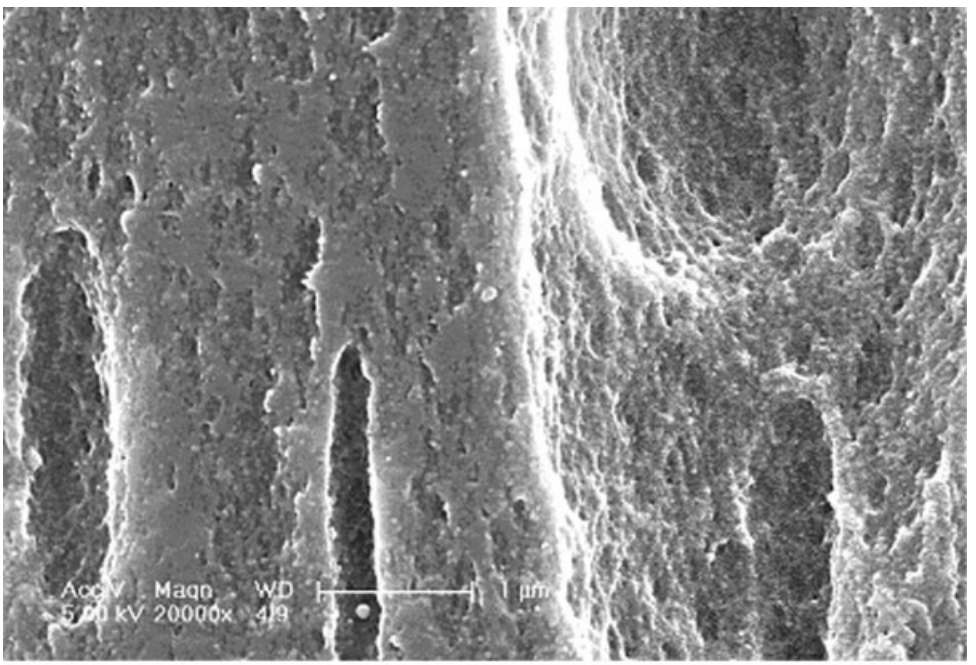

(a)

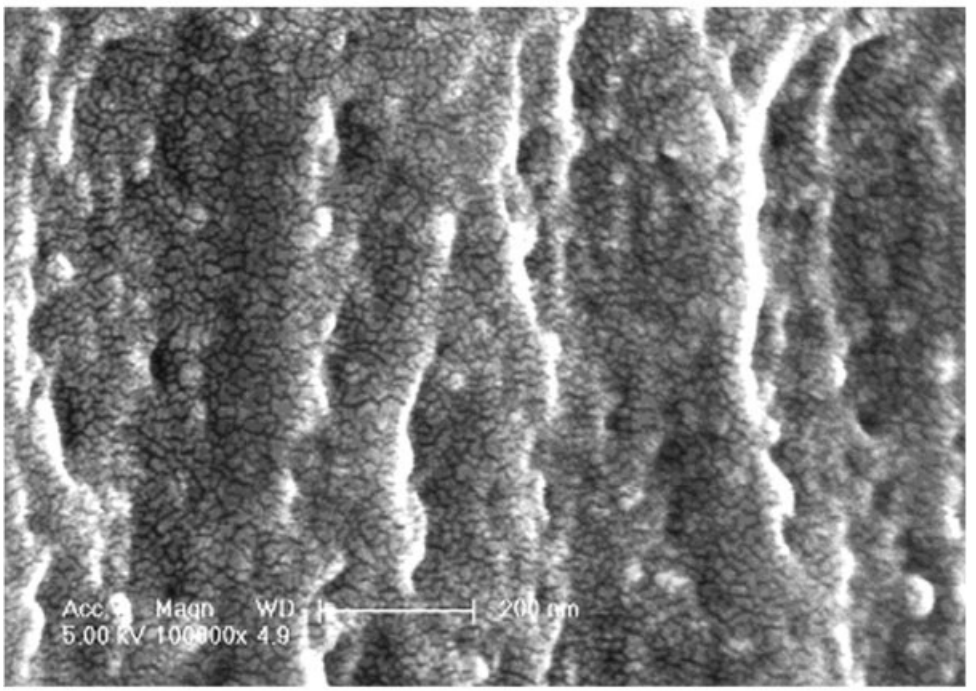

(b)

Figure 5 SEM photos of alkaline hydrolyzed fiber surface for PET/2.0 wt % SiO_2.

NaOH and the micropits were lengthened along the fiber's axis direction, as shown in Figure 4(a,b). As expected, SiO_2 nanoparticles along with the PET fell from the surface of the fibers. Therefore, there were lots of not only micropits but also nanopits on the surface of PET/2.0 wt % SiO_2 fiber during the alkaline hydrolysis process, as shown in Figure 5(a,b). It could be found that the pores became deeper and finer and were characterized by larger specific surface area.

Disperse dye dyeing

Color strength is a term used to describe shade depths of fibers dyed with a disperse dye, which is repre-

TABLE IV
Effects of Hydrolysis Time and SiO_2 Content on the *K/S* Value for PET Fibers

Sample	Hydrolysis time (min)	*K/S* value
Pure PET	0	22.9
	20	24.2
PET/0.1 wt % SiO_2	0	24.9
	20	26.2
PET/0.5 wt % SiO_2	0	25.7
	20	27.1
PET/2.0 wt % SiO_2	0	26.4
	20	31.1

sented by the *K/S* value. In this study, measurements of the *K/S* values of PET fibers could serve as a probe in following fiber structural changes as SiO_2 content changes. The effects of the alkaline hydrolysis time and SiO_2 content on the *K/S* values of pure PET and PET/SiO_2 fibers are listed in Table IV. It could be seen that the *K/S* value of nonhydrolyzed PET fibers increased with increasing SiO_2 content. The difference in *K/S* values of nonhydrolyzed fibers is mainly ascribed to the presence of SiO_2 nanoparticles which resulted in the increase of void spaces necessary for penetration of the disperse dye from the surface into the interior of the fiber.[29,30] These different *K/S* values could be used to reflect the dye uptake. In contrast, the *K/S* values of hydrolyzed fibers were also obtained. After alkaline hydrolysis for 20 min, a large number of pits were produced and tough fiber surface formed. The tough surface facilitated the adsorption of disperse dye at the fiber surface and diffused the reflection to a great extent. Consequently, the color shade deepened and the *K/S* values of all fibers increased. However, the increase in *K/S* value of PET/SiO_2 fibers after hydrolysis is higher than that of pure PET fibers, which is mainly attributed to the tougher superfine structure, such as such as cracks, craters, and cavities. The increase in *K/S* value varied in the order pure PET < PET/0.1 wt % SiO_2 < PET/0.5 wt % SiO_2 < PET/2.0 wt % SiO_2. For example, the *K/S* values of PET/2.0 wt % SiO_2 fibers, hydrolyzed and nonhydrolyzed, are 6.9 and 3.5 *K/S* larger than those of pure PET fiber, as shown in Table IV.

CONCLUSIONS

In this study, PET/SiO_2 nanocomposites prepared by *in situ* polymerization were melt spun into fibers. A homogenous dispersion of SiO_2 nanoparticles and a good adhesion with the PET matrix were obtained. The thermal, mechanical, and dyeable properties of the PET/SiO_2 fibers were investigated. According to the DSC results, it is found that the SiO_2 nanoparticles might act as a marked nucleating agent promoting the crystallization of the PET matrix from melt. The PET/0.1 wt % SiO_2 fibers had a higher tensile strength than pure PET fibers. The rate of hydrolysis increased in the order pure PET < PET/0.1 wt % SiO_2 < PET/0.5 wt % SiO_2 < PET/2.0 wt % SiO_2, pure PET showing slowest loss in weight during the whole treatment process. For the Disperse Blue used, the color strength of the dyeing generally increased with increasing SiO_2 content and hydrolysis time. This could be contributed to the shorter and convenient diffusional path produced by SiO_2 nanoparticles within the PET substrates and the tougher fiber surface. The *K/S* values of PET/2.0 wt % SiO_2 fibers, hydrolyzed and nonhydrolyzed, were 6.9 and 3.5 *K/S* larger than those of pure PET fibers. It is obvious that the deep shade of Disperse Blue dyeing was achieved.

References

1. Bird, C. L. J Soc Dyers Colour 1956, 72, 343.
2. Choi, T. S.; Shimizu, Y. Dyes Pigments 2001, 50, 55.
3. Joung, S. N. J Chem Eng Data 1998, 43, 9.
4. Shashin, M. M. Polym Test 1995, 14, 243.
5. Needles, H. L.; Park, M. J. J Appl Polym Sci 1996, 59, 1683.
6. Bendak, A.; Elmarsafi, S. Ann Chim Rome 1991, 81, 141.
7. Shukla, S. R.; Hundekar, R. V.; Saligram, A. N. J Soc Dyers Colour 1991, 107, 407.
8. Kim, J. P.; Burkinshaw, S. M. J Appl Polym Sci 1993, 49, 1647.
9. Stinson, R. M.; Obendorf, S. K. J Appl Polym Sci 1996, 62, 2121.
10. Aitken, D.; Burkinshaw, S. M. J Soc Dyers Colour 1992, 108, 219.
11. Shukla, S. R.; Mathur, M. R. J Soc Dyers Colour 1997, 113, 178.
12. Thakore, K. A.; Smith, C. B.; Hite, D. Am Dyest Rep 1990, 79, 21.
13. Saligram, A. N.; Shukla, S. R.; Mathur, M. J Soc Dyers Colour 1993, 109, 263.
14. Shimizu, Y.; Yamamoto, R.; Shimizu, H. Textile Res J 1989, 59, 684.
15. Shukla, S. R.; Mathur, M. J Soc Dyers Colour 1995, 111, 342.
16. Wan, A. W. Y.; Lomas, M. J Soc Dyers Colour 1996, 112, 245.
17. Knittel, D.; Saus, W.; Schollmeyer, E. J Fibre Text Res 1997, 22, 184.
18. Santos, W. L. F.; Porto, M. F. J Supercrit Fluid 2001, 19, 177.
19. Kansy, J.; Consolati, G.; Dauwe, C. Phys Chem 2000, 58, 427.
20. Petrovis, Z. S.; Javmi, I.; Waddon, A.; Banhegi, G. J Appl Polym Sci 2000, 76, 2272.
21. Rong, M. Z.; Zhang, M. Q.; Zheng, Y. X.; Zeng, H. M. Polymer 2001, 42, 3301.
22. Chan, C. M.; Wu, J. S.; Li, J. X.; Cheung, Y. K. Polymer 2002, 43, 2981.
23. Zhao, J.; Song, R.; Zhang, Z.; Ling, X. H.; Fan, Q. Macromolecules 2001, 34, 343.
24. Dave, J.; Kumar, R.; Srivastava, C. H. J Appl Polym Sci 1987, 33, 455.
25. Namboori, C. G. S.; Haith, M. S. J Appl Polym Sci 1999 1968, 12.
26. Betschewa, R.; Wangelov, P. Melliand Textilber 1989, 70, 599.
27. Grancaric, A. M.; Kallay, N. J Appl Polym Sci 1993, 49, 175.
28. Zeronian, S. H.; Collins, M. J Text Inst 1989, 20, 1.
29. McGregor, R.; Peters, R. H. J Soc Dyers Colour 1965, 81, 393.
30. Murray, A.; Mortimer, K. J Soc Dyers Colour 1971, 87, 173.